Project Description

The immune system in higher organisms is composed of individual cells called leukocytes which work together to combat pathogens such as bacteria and viruses. These cells are unique because they move throughout the body and signal to each other in order to organize a response to an infection. Upon detecting pathogens in the body, an immune cell will secrete cytokines which are proteins that mediate communication among leukocytes and coordinate their response. Some cytokines called chemokines direct the motion of immune cells along their concentration gradient by a process known as chemotaxis. Other cytokines such as tumor necrosis factor (TNF) recruit cells to the site of inflammation and activate immune cells. One process by which inflammation is regulated is the shedding of cytokine receptors, such as those for TNF (sTNFr). Those soluble receptors bind to the respective cytokines and limit their activity. Based on these signals, the cells will group together to respond to an infection. The ability of these cells to organize spatially in a timely manner is vital to an effective immune response.

Section 1 describes a mathematical model of cytokines and immune cell motion proposed by Kepler in [10] and [11]. The cytokines are modeled continuously as soluble factors governed by reaction-diffusion equations in a three-dimensional domain with source terms that are centered on activated leukocytes. The motion of the immune cells is inherently stochastic, but is biased toward the chemical gradients of the chemokines. In [14], Lucas showed that the solution to this model exists for all time; to be sure, it was necessary to modify the source terms in Kepler's model slightly, as indicated below, for mathematical reasons. We discuss the numerical solution of this system using operator splitting with a multigrid diffusion solver. As is shown in [14], this method succeeds in replicating interesting biological phenomena, albeit for problems of small size and at low resolution. In order to deal with more realistic problem sizes and to obtain better resolution, new methods are necessary.

In section 2 we describe these new methods. We begin by revising the immunology model to more closely reflect the biology. The source terms in the reaction-diffusion equations are replaced by boundary conditions that represent the flux of chemokines through each individual cell surface. Moreover, by expressing the solution to the diffusion equation as a layer potential we can reduce the problem to an integral equation on the boundary. The solution of the two-dimensional integral equation and the evaluation of the layer potentials will be significantly faster than the multigrid scheme in three dimensions. While the approach is straightforward when the immune cells are far apart, we will need to develop new ideas to tackle the problem when the cells get close together or touch. Finally, having solved this problem, we will attempt to incorporate more complex cellular conglomerations such as the formation of granuloma around bacteria.

The proposed work is a collaboration with the Duke University Center for Computational Immunology. A major part of the work of the Center is to use simulation to develop more effective vaccines against harmful bacteria. A significantly improved numerical scheme for the diffusion based on boundary integral methods will allow us to visualize the dynamics of the cytokines and the motion of the cells with high accuracy in real time. Part of the mission

of the Center is to make available to the biological community codes that will simulate the behavior of immune cells.

1 The Current Immunology Model

1.1 Soluble Factors

Suppose $U_i(x,t)$ is the local concentration of soluble factor i at the position x and time t. Let x_α be the position of the center of cell α in the bounded domain $\Omega \in \mathbb{R}^3$. Then for $x \in \Omega$, the reaction-diffusion equations that describe the behavior of the soluble factors from [10, 11] are

$$\begin{aligned}\frac{\partial U_i}{\partial t}(x,t) = &\left\{\eta_i \Delta - \sum_{j=1}^{N} r_{ij} U_j(x,t) - \lambda_i\right\} U_i(x,t) \\ &+ \sum_{\alpha=1}^{M} J_{i\alpha}(x,t) g_\alpha(x - x_\alpha(t)), \quad x \in \Omega, \quad i = 1, \ldots, N.\end{aligned} \tag{1}$$

where $g_\alpha(x)$ is a smoothly cut-off Gaussian with support over the volume of the cell. Here η_i denotes the diffusion coefficient for soluble factor U_i, r_{ij} is the rate at which U_i is removed by interaction with U_j, and λ_i is the rate of removal of U_i by other factors. The secretion of soluble factor U_i by cell α is a Gaussian source centered at the cell position x_α with secretion rate $J_{i\alpha}$. The source term in (1) is a sum over the M individual cells indexed by α. The constants η_i, r_{ij}, and $J_{i\alpha}$ are all positive.

Here we consider a smooth source term with compact support as opposed to the point sources in [10, 11] for two reasons. Point sources do not take into account the volume of the cells which can vary in size and shape. Also, the point sources in [10, 11] are delta functions and we are currently unaware of any rigorous mathematical treatment of (1) with this type of source. We have made use of the smoothness of the source terms in order to show the existence of a solution.

1.2 Cell Motion

The system (1) is coupled with M systems of stochastic differential equations that describe the motion of each individual cell. For each cell, indexed by α, let $x_t \in \mathbb{R}^3$ be the position, $v_t \in \mathbb{R}^3$ be the velocity and $X_t = (x_t, v_t)$. The motion of each cell is a Langevin process

$$\begin{aligned} dx_t &= v_t dt, \\ dv_t &= [h(U(x_t)) - \gamma v_t]\, dt + \sigma(U(x_t))\sqrt{\gamma} dW_t \end{aligned} \tag{2}$$

where dW_t is standard Brownian motion in $\mathbb{R}^3$. The cell velocity is stochastic but biased toward the direction of the gradients of the relevant soluble factors by the relation

$$h(U) = \sum_{i=1}^{N} \frac{\chi_i \nabla U_i}{h_0 + |\nabla U_i|}. \tag{3}$$

Here χ_i is the chemotactic constant that controls how much the drift is influenced by the gradient of soluble factor i and h_0 is the length of the gradient of i at which h attains half its maximum value. The magnitude of the diffusion depends on the concentration by

$$\sigma(U) = \sigma_0 \left(1 + \frac{U}{U_0}\right)^q e^{-\lambda U}. \tag{4}$$

The constants $\gamma, \chi_i, h_0, \sigma_0, u_0, \lambda$ and q are assumed to be positive.

In [14] Lucas showed that the solution to the reaction-diffusion system (1) with a nonnegative initial condition is positive, and the suprema of the solution and its derivatives are *a priori* for finite time. In addition, we have shown that the solution to the full system (1),(2) exists and is well behaved for all time.

1.3 Operator Splitting and Numerical Schemes

We numerically solve the reaction-diffusion-stochastic system (1), (2) by using operator splitting. Consider the following three problems; numerical methods for the solution of each of these are well known:

1. The diffusion of the soluble factors,

$$\frac{\partial U_i}{\partial t}(x,t) = \eta_i \Delta U_i + \sum_{\alpha=1}^{M} J_{i\alpha}(x,0) g_\alpha(x - x_\alpha(0)), \quad i = 1, \ldots, N, \qquad U(0) = u. \tag{5}$$

2. The reactions of the soluble factors,

$$\frac{dU_i}{dt} = -\left\{\sum_{j=1}^{N} r_{ij} U_j(x,t) + \lambda_i\right\} U_i(x,t), \quad i = 1, \ldots, N, \qquad U(0) = u. \tag{6}$$

3. The motion of the cells,

$$\begin{aligned} dx_t &= v_t dt, \quad x(0) = \xi. \\ dv_t &= [h(u(x_t)) - \gamma v_t]\, dt + \sigma(u(x_t))\sqrt{\gamma} dW_t, \quad v(0) = \nu. \end{aligned} \tag{7}$$

Let $t_0, t_1, \ldots, t_n, \ldots$ be a sequence of times such that $t_{n+1} - t_n = \Delta t$. Define $Y(t_n) = (y(t_n), w(t_n))$ and suppose that $(V(t_n), Y(t_n))$ is a given approximation to the solution $(U(t_n), X(t_n))$ to the system (1),(2). Let $u(x) = V(t_n)$ be the given concentrations, $\xi_\alpha = x_\alpha(t_n)$ be the given positions, and $\nu_\alpha = w_\alpha(t_n)$ be the given velocities. We can approximate $U_i(x, t_{n+1})$, $x_\alpha(t_{n+1})$ and $v_\alpha(t_{n+1})$ by the following splitting scheme:

1. Solve the diffusion, (5), for Δt using the initial data $u_i(x)$, and ξ_α and ν_α.
2. Solve the reaction, (6), for Δt using the the solution from the previous step as well as ξ_α and ν_α as initial data.

3. Move the cells according to (7) for one time step Δt using the soluble factors from the previous step as well as ξ_α and ν_α as initial data.

It is well known for reaction-diffusion equations, that the error due to the splitting is $\mathcal{O}(\Delta t)$. (See [8].) The following theorem from [14] extends this result to the reaction-diffusion-stochastic system.

Theorem 1.1. *Let (U, X) be the solution of the system (1), (2) on $[0, T)$ where $(U, X)(0) = (u, \xi)$. Let $(V, Y)(t)$ be the split scheme described above. Then for a nonnegative integer k or $k = \infty$,*

$$\sup_{0\le t\le \Delta t} \left|\mathbb{E}\left[\|U(t) - V(t)\|_k + X_t - Y_t\right]\right| \le C(\sup|u|, \|u\|_{(k+2)\vee 3})(\Delta t)^2. \tag{8}$$

and

$$\sup_{0\le t\le \Delta t} \mathbb{E}\left[\|U(t) - V(t)\|_k + |X_t - Y_t|^2\right]^{\frac{1}{2}} \le C(\sup|u|, \|u\|_{(k+2)\vee 3})(\Delta t)^{\frac{3}{2}}. \tag{9}$$

Using techniques from [16], Lucas has shown that the estimates above lead to a first order method in [14]. There are known numerical methods of solution for each of the three problems listed above. We are currently unaware of any second order splitting methods for systems that contain stochastic differential equations. Strang splitting is a widely used second order method for reaction-diffusion equations, (see [8]), but due to the fact that Itô integrals are of order $\sqrt{\Delta t}$, any time step of order Δt will incur a local truncation error that is of order $(\Delta t)^{\frac{3}{2}}$.

We can discretize the set of decoupled diffusion equations (5) using linear tetrahedral finite elements. This leads to a set of ordinary differential equations of the form

$$M\dot{U}_i^h(t) + A_h U_i^h(t) = MG_i^h(t) \tag{10}$$

where $U_i^h(t)$ and $G_i^h(t)$ are the projections of $U_i^h(t)$ and $\sum_\alpha J_{i\alpha}(x, 0)g_\alpha(x - x_\alpha(0))$ onto the finite element space with mesh width h, respectively. It has been shown in [3] that the resulting error is $\mathcal{O}(h^2)$, The matrices M and A_h are the mass and stiffness matrices that result from the integration of each of the basis elements and the gradients of the basis elements against each other. There are several options to discretize (10) in time. The backward Euler scheme is given by

$$(M + \Delta t A)U_i^{h,n+1} = M\left(U_i^{h,n} + \Delta t G_i^{h,n}\right). \tag{11}$$

Using maximum norm estimates from [18] and [19] and techniques from [22], Lucas has shown that this is a first order method in [13]. Since this scheme requires a linear solve with a poorly conditioned matrix, we use a multigrid scheme. The computational work for multigrid is $\mathcal{O}(N)$ where N is the number of grid points.

Since the reaction equations (6) do not depend on space, we can treat them as a system of ordinary differential equations at each grid point. Consider the semi-implicit discretization of the reaction:

$$\frac{U_i^h(t + \Delta t) - U_i^h(t)}{\Delta t} = -\left(\lambda_i + \sum_{j\ne i} r_{ij}U_j^h(t)\right)U_i^h(t + \Delta t); \tag{12}$$

solving for $U_i^h(t+\Delta t)$, we obtain

$$U_i^h(t+\Delta t) = \frac{U_i^h(t)}{1+\Delta t\left(\lambda_i + \sum_{j\neq i} r_{ij} U_j^h(t)\right)}. \tag{13}$$

It is immediately clear that this method preserves positivity, i.e. if $U_i^h(t) > 0$, then $U_i(t+\Delta t) > 0$ and it is obvious that it is a first order method.

We approximate the cell motion (7) by holding the concentrations fixed at the initial value, i.e.

$$\begin{aligned} \bar{x}_t(\xi) &= \xi + \int_0^t \bar{v}_s ds \\ \bar{v}_t(\nu) &= \nu + \int_0^t \left[h(u(\xi)) - \gamma \bar{v}_s\right] ds + \sqrt{\gamma}\int_0^t \sigma(u(\xi)))dW_s; \end{aligned} \tag{14}$$

here $\bar{x}_t$ and $\bar{v}_t$ are the computed positions and velocities, respectively. Lucas has shown in [13] that the resulting error is $\mathcal{O}(\Delta t)$. Note that we can solve (14) using an integrating factor. Therefore, we can simulate (14) exactly using techniques from [12]. The means of $\bar{x}_t$ and $\bar{v}_t$ are

$$\mu_{\bar{x}} = \xi + \frac{1-e^{-\gamma t}}{\gamma}\nu + \frac{h(u(\xi))}{\gamma^2}(\gamma t - 1 + e^{-\gamma t}), \tag{15}$$

$$\mu_{\bar{v}} = e^{-\gamma t}\nu + \frac{h(u(\xi))}{\gamma}(1-e^{-\gamma t}), \tag{16}$$

and the covariance matrix is given by

$$\Sigma_{\bar{x}\bar{x}} = \frac{1}{\gamma}\left[t - \frac{2}{\gamma}(1-e^{-\gamma t}) + \frac{1}{2\gamma}(1-e^{-2\gamma t})\right] \tag{17}$$

$$\Sigma_{\bar{x}\bar{v}} = \frac{1}{2\gamma}\left(1-e^{\gamma t}\right)^2 \tag{18}$$

$$\Sigma_{\bar{v}\bar{v}} = \frac{1}{2\gamma}\left(1-e^{-2\gamma t}\right). \tag{19}$$

Let Z_1 and Z_2 be independent standard normal distributions. Then the distributions of $\bar{x}_t$ and $\bar{v}_t$ are given by

$$\begin{aligned} \bar{x}_t &= \mu_{\bar{x}} + Z_1\frac{\Sigma_{\bar{x}\bar{v}}}{\sqrt{\Sigma_{\bar{v}\bar{v}}}} + Z_2\sqrt{\Sigma_{\bar{x}\bar{x}} - \frac{\Sigma_{\bar{x}\bar{v}}^2}{\Sigma_{\bar{v}\bar{v}}}} \\ \bar{v}_t &= \mu_{\bar{v}} + Z_1\sqrt{\Sigma_{\bar{v}\bar{v}}}. \end{aligned} \tag{20}$$

Lucas has shown in [13] that the numerical methods described above can be combined to make a first order method for the entire simulation. These methods have been implemented in a simulation program that is described in [17]. The simulations have reproduced the experimental behavior of cells moving stochastically toward sources of chemokines as shown in Figure 1.1.

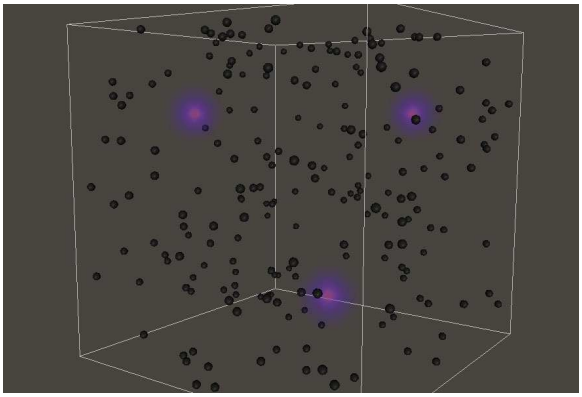

(a) Concentration of MCP1 at $t = 10$min

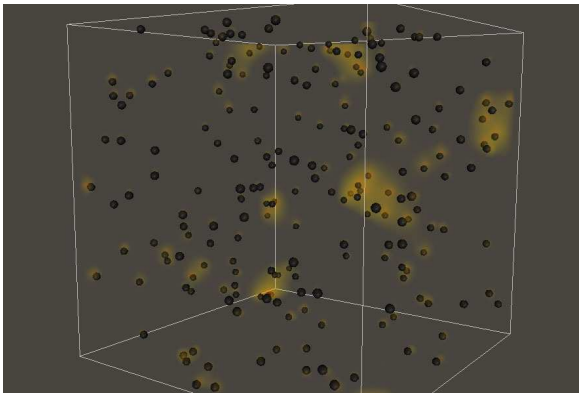

(b) Concentration of TNF at $t = 10$min

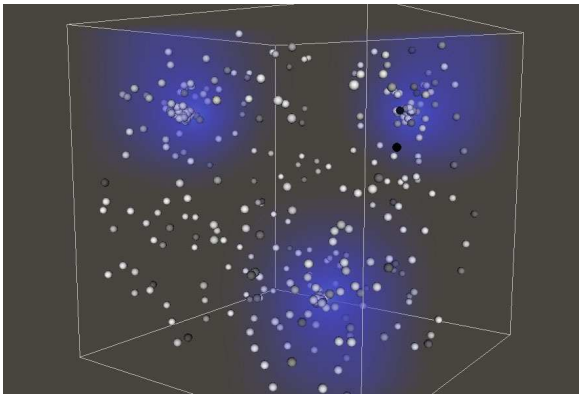

(c) Concentration of MCP1 at $t = 120$min

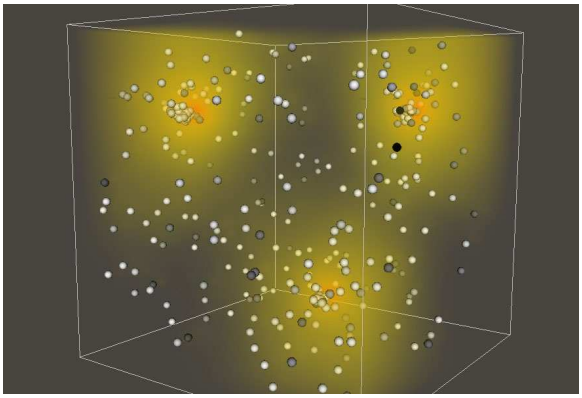

(d) Concentration of TNF at $t = 120$min

Figure 1.1: Simulation of an immune response to three sources of MCP1. Immune cells are colored from black to white by their gene expression.

1.4 Performance

The numerical schemes outlined above have been implemented in C++. The diffusion scheme runs in parallel using MPI (Message Passing Interface). We also have an earlier version of the simulation that includes simple cells moving in parallel and we are working to update the current simulation with more biologically complex cells to run in parallel.

Our current test simulation shows the immune response to three sources of MCP1 which is known to attract immune cells called macrophages. The macrophages secrete TNF and sTNFr depending on their internal state. The domain is a cube with side length 400μm and the radius of each macrophage is 5μm. A simulation with grid spacing 6.25μm, time step 0.1min, and on the order of a thousand cells takes 75 minutes to run 1200 time steps. In Figure 1.4 you can see the cells clustering around the sources of MCP1 after 120min. Within the simulation approximately 93% of the time is spent solving the diffusion. In contrast only 6.25% is spent solving the reaction and less than 0.5% is spent moving the cells, updating their states and resolving collisions.

The computational work for multigrid is proportional to the number gridpoints which for this three-dimensional domain is $(2^6)^3 = 2^{18}$ gridpoints. The same simulation with grid spacing 3.125μm and $(2^7)^3 = 2^{21}$ takes approximately 13 hours to run. Note that the simulation with 2^3 times more gridpoints takes approximately 10 times longer. Since there are three soluble factors and several computational arrays required for the multigrid scheme, this is the upper limit on memory for a desktop machine. A cluster with 64 nodes can increase the number of gridpoints to 2^{27} which translates to a grid spacing of 0.78125μm. In order to resolve the soluble factors accurately we estimate that we will need a grid spacing of less than 0.5μ. This will require a larger cluster in which case communication between nodes will increase the computational time of the simulation. This demonstrates the need for a significantly faster method for solving the diffusion.

1.5 Other Computational Immunology Models

There are three related computational models that simulate multiple cells interacting in a dynamic environment for immune simulation. The first is Compucell [9, 4] from the Interdisciplinary Center for the study of Biocomplexity at the University of Notre Dame. (`http://www.nd.edu/~lcls/compucell/`) This model also uses a set of reaction-diffusion equations to model chemical concentrations in a three-dimensional domain. In contrast to the Kepler model, the immune cells are modeled as a cellular automata whose dynamics depend on minimizing the total effective energy of the system. The appeal of this model is limited to experimental immunologists, since it is difficult to relate the simulation to detailed biological mechanisms.

Simmune [15] is developed at the National Institute of Allergy and Infectious Disease. (`http://www3.niaid.nih.gov/labs/aboutlabs/psiim/computationalBiology/`) This is also an agent-based model that contains cell types that closely model the underlying biology. The focus of the project is on the biochemistry rather than the biophysics of cell motility and diffusion from a motile source.

Finally, the Bray Group at the University of Cambridge focuses on computational models of bacterial chemotaxis. (`http://www.pdn.cam.ac.uk/groups/comp-cell/`). For example, the model in [2] focuses on cell behavior in response to fixed two-dimensional gradients. Although the cell models are detailed, there are no cytokine kinetics and the domain is only two-dimensional.

The advantage of the using the reaction-diffusion-stochastic model (1), (2) is that it contains realistic agents that respond to cytokines in a three-dimensional domain. To approximate the dynamics of the soluble factors, we either require large amount of computing time or a faster numerical method for solving the reaction-diffusion equations.

2 Revision of the Immunology Model

In addition to the performance concerns previously outlined, one criticism of the soluble factors model with source terms (1) is that it does not take into account the volume of the cells. In this model the dynamics of the soluble factors are not affected by the boundaries

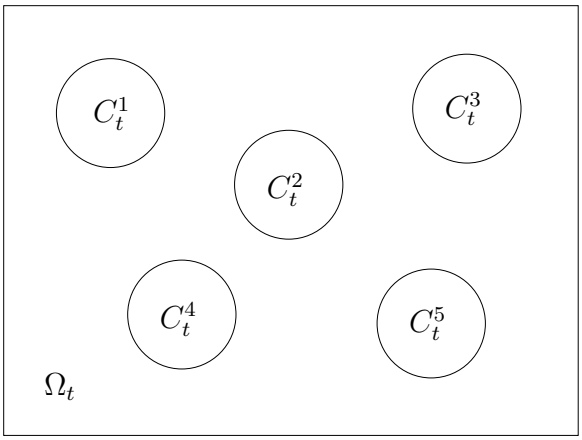

Figure 2.1: The domain Ω_t with cell boundaries.

of the cells and the domain is considered to be an empty space with no obstructions. In reality, the reaction-diffusion equations are not valid inside the cells. Also, the cell secretion behavior is more accurately described by a flux through the surface of the cell α at a rate $J_{i\alpha}(x,t)$. Let C_t^α be the space occupied by cell α and define

$$\Omega_t = \mathcal{U} - \sum_\alpha C_t^\alpha$$

where $\mathcal{U} \in \mathbb{R}^3$ is bounded. Figure 2.1 shows a sample domain Ω_t. If ∂C_t^α denotes the surface of cell α, then the secretion of soluble factor i by cell α is given by the boundary condition

$$\eta_i \partial_{n_t(x)} U_i(x,t) = J_{i\alpha}(x,t), \quad x \in \partial\Omega_t^\alpha \tag{21}$$

where $n_t^\alpha(x)$ is the outward unit normal from the surface ∂C_t^α. These observations lead to the initial boundary value problem

$$\begin{aligned}
\frac{\partial U_i}{\partial t}(x,t) &= \left\{ \eta_i \Delta - \sum_{j=1}^N r_{ij} U_j(x,t) - \lambda_i \right\} U_i(x,t) && x \in \Omega_t, \quad i = 1, \ldots, N, \\
U_i(0) &= u_i(x) && x \in \bar{\Omega}_0, \\
\eta_i \partial_{n_t(x)} U_i(x,t) &= J_{i\alpha}(x,t), && x \in \partial C_t^\alpha, \quad 1 \le \alpha \le M.
\end{aligned} \tag{22}$$

Although the shapes of the immune cells can be complex, as a first approximation we will consider the cells to be spheres. Again we will prove the existence of a solution to the system (22),(2) using ideas already developed in [14]. We will also show that the solution to the reaction-diffusion equations (22) are positive given non-negative initial conditions.

2.1 Numerical Schemes for the Diffusion

To solve the system numerically we will use operator splitting as before. The equations and the numerical schemes for the reaction and cell motion are the same as previously outlined.

The boundaries of the cells are held fixed for the diffusion, i.e $\Omega = \Omega_{t_n}$, $C^\alpha = C^\alpha_{t_n}$, and $\partial^\alpha_{n(x)} = \partial^\alpha_{n_{t_n}(x)}$. As before, let $t_0, t_1, \ldots, t_n, \ldots$ be a sequence of times such that $t_{n+1} - t_n = \Delta t$. The initial boundary value problem for the diffusion of a single soluble factor U with diffusion coefficient η for $t_n \le t \le t_{n+1}$ is

$$\begin{aligned} \frac{\partial U}{\partial t}(x,t) &= \eta \Delta U(x,t), && x \in \Omega \\ U(x,t_n) &= u(x), && x \in \bar{\Omega}, \\ \eta \partial_{n(x)} U(x,t) &= J_\alpha(x,t), && x \in \partial C^\alpha, \end{aligned} \tag{23}$$

where $\Omega \in \mathbb{R}^3$ is a bounded domain that does not include the volume of each cell. We can proceed using layer potentials. Assume that the solution is of the form

$$U(x,t) = S\mu(x,t) + Lu(x), \quad x \in \Omega, \quad t > 0. \tag{24}$$

where $S\mu$ is called the *single layer potential*,

$$S\mu(x,t) = \int_0^t \int_{\partial\Omega} k_{t-\tau}(x-z)\mu(z,\tau)\, dz\, d\tau \tag{25}$$

and $k_t(x)$ is the heat kernel,

$$k_t(x) = (4\pi t)^{-\frac{3}{2}} e^{-\frac{|x-y|^2}{4t}}. \tag{26}$$

Let $Q : C^1(\bar{\Omega}) \to C^1_0(\mathbb{R}^3)$ be a linear continuous extension of u such that $Qu(x) = u(x)$ for $x \in \Omega$. Note that Qu is compactly supported. Define

$$Lu(x,t) = \int_{\mathcal{U}} k_t(x-y) Qu(y)\, dy. \tag{27}$$

Then $U(x,t)$ satisfies the differential equation and initial condition in (23). It has been shown in [5] that for $w \in \partial\Omega$,

$$\lim_{x \to w} \partial_{n(x)} U = \frac{1}{2}\mu(w,t) + D\mu(w,t) \tag{28}$$

where

$$D\mu(x,t) = \int_0^t \int_{\partial\Omega} (\partial_x)_{n(x)} k_{t-\tau}(x-z)\mu(z,\tau)\, dz\, d\tau \tag{29}$$

is called the *double layer potential*. Substituting $U = S\mu$ into the boundary condition in (23) leads to the Volterra integral equation of the second kind

$$\frac{1}{2}\mu(w,t) + D\mu(w,t) = \frac{1}{\eta} J(w,t) - Mu(w), \quad w \in \partial\Omega, \tag{30}$$

where

$$\begin{aligned} Mu(x) &= \int_{\mathcal{U}} (\partial_x)_{n(x)} k_t(x-y) Qu(y)\, dy \\ &= \int_{\mathcal{U}} k_t(x-y) (\partial_y)_{n(x)} Qu(y)\, dy. \end{aligned}$$

Note that Mu is $\mathcal{O}(1)$ in t. Therefore, solving the diffusion numerically involves two steps:

1. Solve the integral equation (30).

2. Evaluate the integrals in (24).

We note that both of these steps are essentially two dimensional problems. The single and double layer potentials both contain integrals over the boundary which reduces the dimension of the problem. Although Lu and Mu both contain an integral over the entire domain, the contribution from outside a ball centered at x will be negligible. It is also worth noting that we only need to evaluate (24) within a finite range of each individual cell. This is because the model cells only need the values of the soluble factor concentrations on their boundaries in order to calculate the gradient to determine their direction of motion. These factors will drastically reduce the computational work for the diffusion step.

The solution to the integral equation (30) is given by

$$\mu = \left(\frac{1}{2}I + D\right)^{-1}\left(\frac{1}{\eta}J - Mu\right).$$

To solve the integral equation (30) numerically we note that

$$D\mu(w,t) = \sqrt{\frac{t-t_n}{\pi}}H(w)\mu(w,t) + \mathcal{O}\left((t-t_n)^{\frac{3}{2}}\right), \quad t_n \le t \le t_{n+1}, \tag{31}$$

where $H(w)$ is the mean curvature of $\partial\Omega$ and the constant depends on two derivatives of μ. The existence of such an expansion is asserted in [20] and proved in [21]. We have verified this result independently as well. Then for

$$\bar{\mu}(w,t) = \left(\frac{1}{2} + \sqrt{\frac{t-t_n}{\pi}}H(w)\right)^{-1}, \quad t_n \le t \le t_{n+1}, \tag{32}$$

it follows that

$$\sup_{w,t_n\le t\le t_{n+1}} |\bar{\mu} - \mu| = \mathcal{O}(\Delta t^{\frac{3}{2}}). \tag{33}$$

We also note that

$$\|S\mu\|_\infty \le C\sqrt{\Delta t}\,\|\mu\|_\infty \tag{34}$$

where the constant is independent of μ. It follows from (33) and (34) that the local truncation error is

$$\sup_{w,t_n\le t\le t_{n+1}} |S\bar{\mu} - S\mu| = \sup_{w,t_n\le t\le t_{n+1}} |\bar{\mu} - \mu|\,\mathcal{O}(\sqrt{\Delta t}) = \mathcal{O}(\Delta t^2).$$

Therefore, we have a first order method for the diffusion.

Once we have an approximation for $\mu(x,t)$, we can employ a fast summation method for computing $U(x,t) = S\mu(x,t) + Lu(x)$ described in [6]. This method relies on two different representations of the heat kernel, a sum of Gaussians which converges quickly for small t and Fourier series which converges quickly for large t. In our case, we will solve the diffusion for small time steps Δt and therefore will use the sum of Gaussians to approximate the heat kernel.

2.2 Immune Cells in Close Proximity

It is important to note that the boundary integral method we have just described breaks down when cells get close together. Note that the double layer potential is an integral over the entire boundary which includes the boundary of each cell, i.e.

$$\begin{aligned} D\mu(x,t) &= \int_0^t \int_{\partial\Omega} (\partial_x)_{n(x)} k_{t-\tau}(x-z)\mu(z,\tau)\,dz\,d\tau \\ &= \sum_{\alpha=1}^{M} \int_0^t \int_{\partial C^\alpha} (\partial_x)_{n(x)} k_{t-\tau}(x-z)\mu(z,\tau)\,dz\,d\tau, \quad x \in \Omega. \end{aligned}$$

If x is far from the boundary of cell α, then $k_{t-\tau}(x-z)$ is small and the contribution from the integral over ∂C^α can be ignored. Therefore, if a single cell is isolated from the others, then the integral equation (30) can be solved independently on that cell boundary.

Consider the case where two cells are close together or are touching, but are isolated from the rest of the cells as in Figure 2.2. Then the integral equation (30) becomes

$$\begin{aligned} \frac{1}{2}\mu(w,t) &+ \int_0^t \int_{\partial C^1} (\partial_w)_{n(w)} k_{t-\tau}(w-z)\mu(z,\tau)\,dz\,d\tau \\ &+ \int_0^t \int_{\partial C^2} (\partial_w)_{n(w)} k_{t-\tau}(w-z)\mu(z,\tau)\,dz\,d\tau = \frac{1}{\eta} J(w,t) - Mu(w), \quad w \in \partial\Omega. \end{aligned} \tag{35}$$

For a fixed $w = b \in \partial C^1$, the first integral can be approximated as before using the expansion (31). We have begun the derivation of a useful expansion for the second integral. We have shown that this expansion will be of the form

$$f(b)\mu(c,t) + E\mu(b,t) \tag{36}$$

where c is the nearest point to b on C^2, where f is a simple function depending on the local geometry that is $\mathcal{O}(|b-c|)$ and where E is a well-behaved integral operator which we are

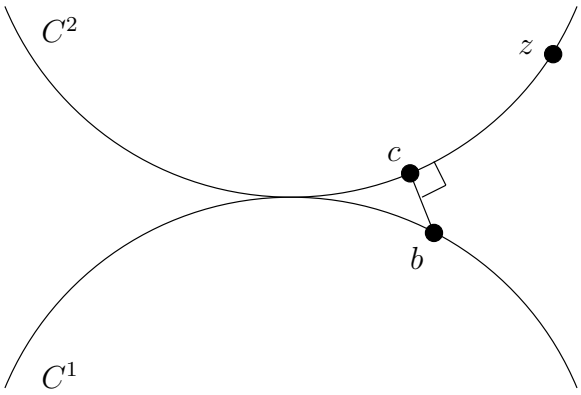

Figure 2.2: Two cells in close proximity.

continuing to study. It is not clear that using the nearest point c on C^2 to b is the best way to proceed. We are studying replacing c with the reflection of b across the plane perpendicular to the midpoints of the two spheres.

2.3 Further Complications to the Model

There are many variations and enhancements of the chemotaxis model we have proposed that will more accurately reflect the biology. We can consider more complex domains that resemble tissue structures in the body. These domains could contain blood vessels and fibrous tissue whose boundaries will also affect the dynamics of the soluble factors. The shapes of the cells themselves are not necessarily spherical and deform as the cells move. The cells also may secrete different cytokines from different locations on their boundaries. In each of these cases we can use the existing theory to solve the diffusion, but the computations themselves will be more complex.

References

[1] Kendall E. Atkinson. *The numerical solution of integral equations of the second kind*, volume 4 of *Cambridge Monographs on Applied and Computational Mathematics*. Cambridge University Press, Cambridge, 1997.

[2] Dennis Bray, Matthew D. Levin, and Karen Lipkow. The chemotactic behavior of computer-based surrogate bacteria. *Current Biology*, 17:12–19, 2007.

[3] Susanne C. Brenner and L. Ridgway Scott. *The mathematical theory of finite element methods*. Springer-Verlag, New York, 2002.

[4] Trevor M Cickovski, Chenbang Huang, Rajiv Chaturvedi, Tilmann Glimm, H. George E Hentschel, Mark S Alber, James A Glazier, Stuart A Newman, and Jess A Izaguirre. A framework for three-dimensional simulation of morphogenesis. *IEEE/ACM Trans Comput Biol Bioinform*, 2(4):273–288, 2005.

[5] Avner Friedman. *Partial Differential Equations of Parabolic Type*. Prentice-Hall, Englewood Cliffs, NJ, 1964.

[6] Leslie Greengard and John Strain. A fast algorithm for the evaluation of heat potentials. *Comm. Pure Appl. Math.*, 43(8):949–963, 1990.

[7] Leslie Greengard and John Strain. The fast Gauss transform. *SIAM J. Sci. Statist. Comput.*, 12(1):79–94, 1991.

[8] Willem Hundsdorfer and Jan Verwer. *Numerical solution of time-dependent advection-diffusion-reaction equations*. Springer-Verlag, Berlin, 2003.

[9] J. A. Izaguirre, R. Chaturvedi, C. Huang, T. Cickovski, J. Coffland, G. Thomas, G. Forgacs, M. Alber, G. Hentschel, S. A. Newman, and J. A. Glazier. Compucell, a multi-model framework for simulation of morphogenesis. *Bioinformatics*, 20(7):1129–1137, May 2004.

[10] Thomas B. Kepler. Microsimulation of inducible reorganization in immunity. In Thomas S. Deisboeck and J. Yasha Kresh, editors, *Complex Systems Science in BioMedicine*, International Topics in Biomedical Engineering, pages 437–450. Springer, New York, 2006.

[11] Thomas B Kepler and Cliburn Chan. Spatiotemporal programming of a simple inflammatory process. *Immunol Rev*, 216:153–163, Apr 2007.

[12] Don S. Lemons. *An introduction to stochastic processes in physics*. Johns Hopkins University Press, Baltimore, MD, 2002. translated by Anthony Gythiel.

[13] Timothy A. Lucas. Numerical solutions of an immunology model using reaction-diffusion equations with stochastic source terms. (In preparation).

[14] Timothy A. Lucas. Operator splitting for an immunology model using reaction-diffusion equations with stochastic source terms. *SIAM J. Numer. Anal.* (Submitted).

[15] Martin Meier-Schellersheim, Xuehua Xu, Bastian Angermann, Eric J Kunkel, Tian Jin, and Ronald N Germain. Key role of local regulation in chemosensing revealed by a new molecular interaction-based modeling method. *PLoS Comput Biol*, 2(7):e82, Jul 2006.

[16] G. N. Milstein. *Numerical integration of stochastic differential equations*. Kluwer Academic Publishers Group, Dordrecht, 1995. Translated and revised from the 1988 Russian original.

[17] Faheem Mitha, Timothy A Lucas, Feng Feng, Thomas B Kepler, and Cliburn Chan. The multiscale systems immunology project: Software for cell-based immunological simulation. *Source Code for Biology and Medicine*. (Submitted).

[18] A. H. Schatz, V. Thomée, and L. B. Wahlbin. Stability, analyticity, and almost best approximation in maximum norm for parabolic finite element equations. *Comm. Pure Appl. Math.*, 51(11-12):1349–1385, 1998.

[19] Alfred H. Schatz. Pointwise error estimates and asymptotic error expansion inequalities for the finite element method on irregular grids. I. Global estimates. *Math. Comp.*, 67(223):877–899, 1998.

[20] Johannes Tausch. A fast method for solving the heat equation by layer potentials. *J. Comput. Phys.*, 224(2):956–969, 2007.

[21] Johannes Tausch. Nyström discretization of parabolic boundary integral equations. 2007. (Preprint).

[22] Vidar Thomée. *Galerkin finite element methods for parabolic problems*. Springer-Verlag, Berlin, second edition, 2006.